Bull. Disas. Prev. Res. Inst., Kyoto Univ., Vol. 21, Part 2, No. 189, November, 1971

On the Nature of the Occurrence of Intermediate and Deep Earthquakes

3. Focal Mechanisms of Multiplets

By Kazuo OIKE

(Manuscript received September 10, 1971)

Abstract

The relations between the distribution of the foci of foreshocks and aftershocks and the focal mechanisms of main shocks in twenty-five multiplets have been investigated.

Foreshocks and aftershocks always occur on one of the nodal planes of a main shock. This is explained by the characteristics of a shear fault plane which has a strong tendency to propagate itself.

Considering these properties of multiplets, the slip planes of main shocks are determined from the analyses of the distribution of foci. It is concluded that the slip planes of intermediate and deep earthquakes are generally parallel to the strike of the seismic plane in the regions, and in intermediate earthquakes the cases in which a deeper side block slips down are predominant.

Two doublets with remarkably short time intervals are analyzed in detail and upper limit of the propagating velocity of fractures in deep foci is determined at being 4.7 km/sec.

1. Introduction

Some characteristics of intermediate and deep multiplets have been described in our preceeding paper analyzing statistically the spatial and temporal clustering of intermediate and deep earthquakes. One of these characteristics is that multiplets frequently occur in the restricted regions which correspond to the bent edges or the contortions of the descending lithospheric plates. Another is that the hypocenters of shocks in each multiplet distribute on a long and slender plane which has a proper direction to the region and the largest shock occurs at the end of the distribution. It has been suggested that there are some relations between such distribution of foci in each multiplet and the earthquake generating stresses at the focal region (Oike, 1971).[1)]

The purposes of the present study are to investigate in detail the characters of each multiplet and to clarify the relation between the distribution of foci of foreshocks and aftershocks and the focal mechanisms of a main shock. The results will give some significant data for discussion of the focal process of intermediate and deep earthquakes.

There have been numerous investigations on the focal mechanisms of intermediate and deep earthquakes. In particular it is generally known that the radiation patterns of P and S waves are explained by a model of the double couple force system. It is often regarded as corresponding to the occurrence of the shear fault at the focal region, but other explanations are of cause possible. For example, such radiation patterns of double couple type are expected from a volumetric souce with sudden change in volume caused by the phase transition (Knopoff and Randall, 1970,[2)] and

Randall and Knopoff, 1970[3]).

From the analyses of focal mechanism solutions, Isacks and Molnar (1969, 1971)[4,5] have concluded that intermediate and deep earthquakes occur within the descending slab of lithosphere and pointed out the close relation between the stress field within the slab and the directions of principal axes of stresses obtained from the fault plane solutions. Results obtained by McKenzie (1969)[6] and Isakcs and Molnar (1969)[7] suggest that intermediate and deep earthquakes are caused by the brittle fracture in the coldest part of the descending slab when the stress prevailing in it surpasses the strength of the lithospere. On the other hand, Fukao (1970)[8], Mikumo (1971)[9], and Abe (1971)[10] studied the source mechanisms of intermediate and deep earthquakes analyzing P, S and surface wave forms and showed that the shear fault model is well fitted to their foci and they determined some significant fault parameters.

From the analyses of the deep multiplets which contain more than two shocks with very short time and space intervals, the shear fault model is also supported. Oike (1969)[11] analyzed the P waves of the large deep earthquake of June 22, 1966, and showed that it was a doublet and the second shock occurred on one of the nodal planes of the first shock. The Peru-Bolivia border earthquake of August 15, 1963, investigated by Chandra (1970)[12] also showed the same characteristics. Fukao (1971)[13] studied the long-period P waves of the western Brazil earthquake of 1963, and showed that this earthquake was a triplet. Two aftershocks with short time intervals also occurred on one of nodal palnes of a main shock and he determined the slip plane of the main shock from it. It has also been described by Isacks et al. (1967)[14] and Santô (1969, 1969, 1970, 1970)[15-18] that there exist many multiplets among intermediate and deep earthquakes.

Spatial distribution of foreshocks and aftershocks of shallow earthquakes have been investigated in detail. For example, Yamakawa (1971)[19] and Yamakawa and Kishio (1971)[20] discovered that large aftershocks distributed on one of the nodal planes of a main shock. Such properties of aftershocks have given many important suggestions to the investigation of the focal process of shallow earthquakes.

Chinnery (1963)[21] computed the change in stress field around the strike-slip fault in a semi-infinite elastic medium, and showed that there were some regions where shearing stresses were not decreased but increased. The fault has a strong tendency to propagate itself. Maruyama (1969)[22] produced many contour maps which showed the stress distribution around a crack, analyzing in detail two-dimensional crack models in a purely elastic homogeneous medium with various boundary conditions on the crack surface. It has been concluded that there are always regions where certain components of stress are not decreased but increased by the introduction of a crack and it is closely related to the mechanism of the occurrence of aftershocks.

2. Stress Field Around a Shear Fault

The distance from the free surface to the focus of a deep earthquake is sufficiently large compared with the dimension of the focal region, and the travel time of the first arrivals at the epicenter is more than several tens of seconds in the case of a deep earthquake. It is more appropriate therefore, to consider a fault plane in an infinite elastic medium to be a source model than to use the results on the fault plane near the surface of a semi-infinite elastic medium or those of a two-dimensional crack model.

In the present investigation the distribution of stresses around an elliptic fault plane in an infinite elastic medium is calculated. The elliptic fault plane is defined by the formula, $x^2/a^2+z^2/b^2=1$, and shear dislocations, $\Delta u(x, z)$, are distributed on it to be maximum at the center and zero along the edge as defined as follows,

$$\Delta u(x, z)=\Delta u_0\sqrt{1-x^2/a^2-z^2/b^2}, \tag{1}$$

where a and b are the semi-axes of the ellipse and Δu_0 is the maximum shear dislocation on the surface of the fault. This equation is taken from Eshelby's (1957)[23] static solution for the discontinuity in displacement across an ellipsoidal cavity in an elastic medium subject to shear stresses, corresponding to the case in which one axis of the ellipsoid approaches zero. It represents the equilibrium slip on a shear fault in which there is no friction between the two faces of the fault. This model has been assumed being a reasonably realistic fault model by Savage (1966)[24] to calculate the seismic wave forms. Coordinates of the fault plane and the distribution of the normalized amplitudes of shear dislocation on the fault are shown in Fig. 1, in the case of $b/a=0.8$.

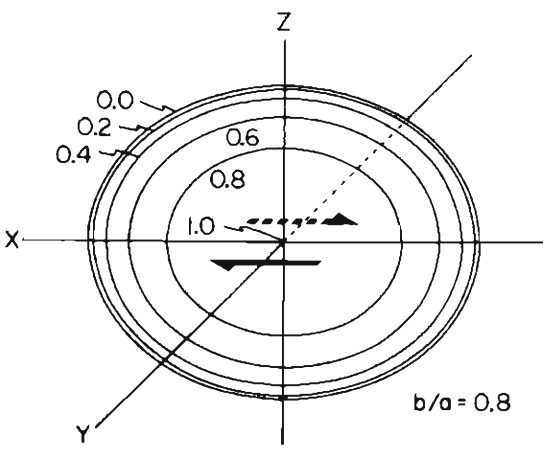

Fig. 1. Coordinates and the distribution of the normalized amplitudes of the shear dislocation on the fault plane.

When X, Y and Z axes in Fig. 1 correspond to x_1, x_2 and x_3 axes and assumed to be $\lambda=\mu$, the stress component τ_{mn} at the point $Q(x_1, x_2, x_3)$ which is not on the fault surface S is described as follows (Maruyama, 1964)[25],

$$\tau_{mn}(Q)=\iint \Delta u\cdot G^{mn}\cdot dS, \tag{2}$$

$$G^{mn}=\frac{\mu}{4\pi}\left\{\frac{2}{3}(\delta_{1m}\delta_{2n}+\delta_{2m}\delta_{1n})\frac{1}{r^3}\right.$$

$$\left.+2\delta_{mn}\frac{r_1r_2}{r^5}\right.$$

$$+(\delta_{1m}r_2r_n+\delta_{2m}r_1r_n+\delta_{1n}r_2r_m+\delta_{2n}r_1r_m)\frac{1}{r^5}$$

$$-20\frac{r_1r_2r_mr_n}{r^7}\Big\}, \qquad (3)$$

where $r_k=x_k-\xi_k, \qquad (k=1, 2, 3),$

for $P(\xi_1, \xi_2, \xi_3)$ on the fault surface S.

Computed results of τ_{xy} are shown in Figs. 2, 3 and 4 for $a=50$ km, $b=40$ km, $\Delta u_0=2$ m and $\mu=3\times10^{11}$ c.g.s. The absolute values of τ_{xy} (dyne/cm^2) are obtained by multipling the values in the figures by 10^5.

The distribution of τ_{xy} on the X-Y plane ($Z=0$) shows a similar pattern to that on the free surface of the semi-infinite medium given by Chinnery (1963)[26]. It is owing to the fact that the sets of symmetrical points to the X-Y plane make image points and the boundary conditions of the free surface are nearly satisfied on the plane. From the distributions shown in Figs. 2 and 3 it is found that there are small regions along the Y-axis where the components of τ_{xy} are not decreased but are slightly increased. In all regions along the edge of the fault plane τ_{xy} are significantly increased as is shown in Fig. 4. Similar results will be obtained even if non-elastic properties of the substance are taken into consideration. It is concluded that a

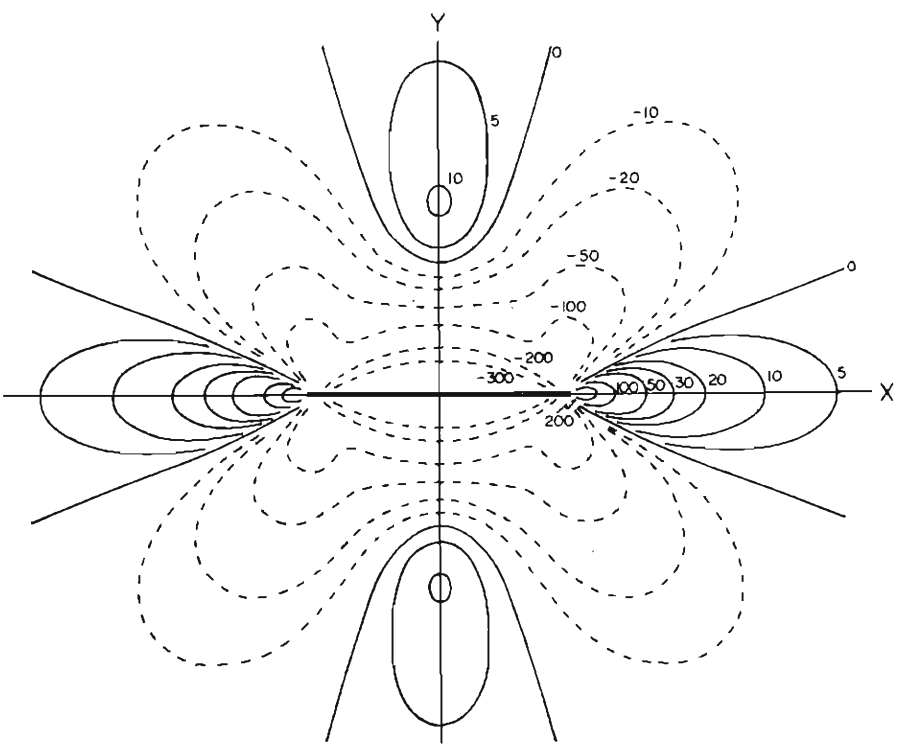

Fig. 2. Distribution of the τ_{xy} on the X-Y plane. A heavy solid line indicates the fault plane. Solid lines and dotted lines indicate the regions where τ_{xy} are increased and decreased, respectively.

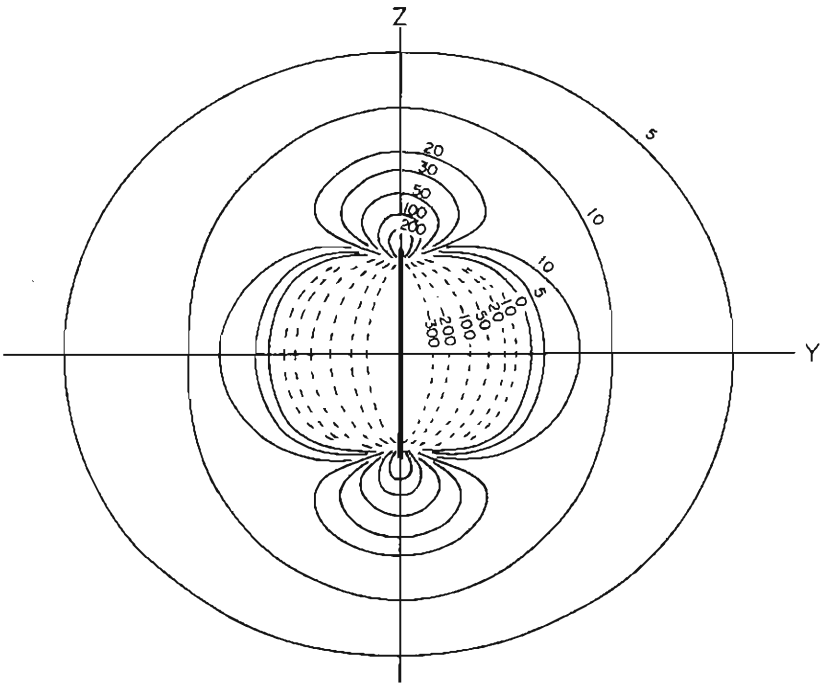

Fig. 3. τ_{xy} on the Y-Z plane. Expressions are same as in Fig. 2.

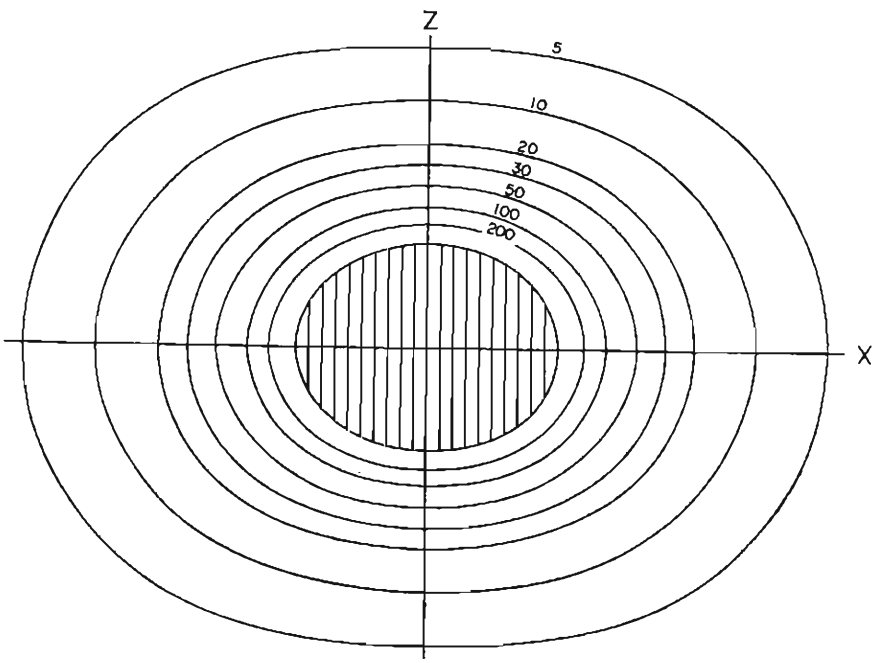

Fig. 4. τ_{xy} on the X-Z plane. Shearing stresses are increased in all regions around the fault.

shear fault in an infinite elastic medium has a strong tendency to propagate itself. If it is assumed that this character is closely related to the occurrence of aftershocks, their foci are distributed along the edge of the fault plane of a main shock. It is conversely concluded that the slip plane of a main shock is determined from the distribution of the foci of aftershocks in the case of multiplets.

Other components of stresses are also increased in some regions especially along the Z-axis. This suggests that the fault plane solutions of aftershocks do not always coincide with that of a main shock.

These results are of cause described only for the change of the stress fields before and after the introduction of a shear fault. The residual stresses after the occurrence of an earthquake may be more complicated corresponding with the initial stress field. A shear fault, however, has more or less the property of propagating itself. It seems to depend upon the state of the materials and the initial stress field in and around the focal region whether the tendency accompaning aftershocks strongly appears or not.

Dynamic wave forms radiated from a shear fault as discussed here have been calculated by Oike (1971)[27] using the Haskell's (1969)[28] method and compared with the records of deep earthquakes containing the ultra-long-period waves (Oike, 1969).[29]

3. Determination of the Space and Time Intervals Between Two Foci

Multiplets have been taken from a list of intermediate and deep earthquakes for the years from 1964 to 1969. Multiplets whose main shocks had a reliable fault plane solutions have been analyzed. Fault plane solutions were adopted from the list of Isacks and Molnar (1971)[30] who selected reliable solutions or newly determined them. For these multiplets the difference between arrival times of initial P waves of two shocks at the same stations were obtained from the reports of iP in the Bulletins of International Seismological Center and the Preliminary Determination of Epicenters of U.S. Coast and Geodetic Survey and from the film copies of long and short-period seismograms of WWSSN. On some multiplets data obtained from the short-period seismograms of microearthquake observation stations in Japan were added. The cases in which data were distributed in a biased direction seen from the foci were excluded.

Twenty-five multiplets selected by the methods above mentioned have been analyzed. The space and time intervals between two foci of each set in a multiplet are determined by the method described by Isacks et al. (1967)[31] and Oike (1969)[32] as follows.

The time difference, τ_j, at the j-th station between arrival times of two initial P waves radiated from two near origins, O_1 and O_2, is described as follows (Fig. 5),

$$\tau_j = t_2 - t_1 - \frac{l}{v_p} \cos \delta_j, \tag{4}$$

where t_1 and t_2 are the origin times of O_1 and O_2, v_p is the P wave velocity around O_1 and O_2 and $\cos \delta_j$ is the direction cosine of ray path for the j-th station to the dire ction of $\overline{O_1O_2}$. τ_j is in proportion to $\cos \delta_j$ and from its relation the space

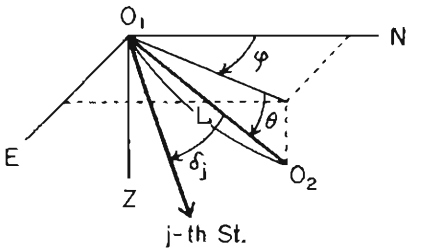

Fig. 5.

interval, l, and the time interval, t_2-t_1, are obtained.

A hundred directions of (θ_i, φ_i) are distributed at approapriate intervals on the lower hemi-focal-sphere, and then for each direction the coefficients of the formula (4) and the standard deviation are calculated by means of least square. Drawing contour lines of equal standard deviation on the stereographic projection of the lower hemisphere, the direction in which the standard devaition is minimum is determined to be the direction of $\overline{O_1O_2}$, and then l and t_2-t_1 are determined from the coefficients. The contour lines of equal standard deviations of doublets and triplets and the directions of the foreshocks and aftershocks are shown in Fig. 6 by the stereographic projection of the lower hime-sphere of each main shock.

Origin time, location, depth and parameters of nodal planes are shown in Table 1 and the calculated results of space and time intervals between each main shock and foreshocks and aftershocks and the direction of their foci seen from each main shock are listed in Table 2. In each multiplet the alphabetical order of shocks corresponds to the sequence of time. In cases that more than two shocks in a multiplet are sufficiently large to obtain the fault plane solutions, results for each shock with the solution are shown.

The accuracy of the results are known from the distribution of the standard deviation in Fig. 6. For the case of l larger than 20 km, the direction is determined within an error of ± 5 degrees. For the shorter distance of l, the accuracy of the direction more or less goes down.

4. Doublets with Remarkably Short Time Intervals

The deep earthquake of June 22, 1966, in the Banda Sea (No. 12 in Table 1) was a doublet containing two shocks which occurred successively with a short time interval (Oike, 1969)[33]. The results calculated adding some data are nearly the same. The second shock occurred on one of the nodal planes of the first shock whose strike was nearly in the north-south direction. Fault plane solutions and the direction of $\overline{O_1O_2}$ are shown in Fig. 7.

The seismic moment of second shock was about four times as large as that of the first (Oike, 1969)[33]. These results show that a dip slip type fault occurred in the first stage and from the lower dege of this fault it propagated downward being a little distorted in the second stage on a larger scale. The point where the second fault plane started to propagate was about 40 degrees from the pole of the fault plane of the first shock.

The deep earthquake of March 31, 1969, in the Sea of Japan (No. 6 in Table 2)

Table1. List of main shocks and their fault plane solutions. Fault planes are determined from the distribution of the foci of aftershocks.

No.	mo.	day	yr.	Time h	m	s	Lat.	Long.	depth	Null Axis trend	plunge	Pole of Fault Plane trend	plunge	Pole of Aux. Plane trend	plunge
							degrees		km						
1 a	Dec.	9	1964	13	35	41.9	27.46S	63.23W	578	171	00	081	12	261	78
2 a	Dec.	27	1967	9	17	55.7	21.20S	68.30W	135	334	07	073	56	239	33
3 a	May	1	1966	16	22	56.3	8.49S	74.25W	165	021	15	148	66	286	19
4 a	Nov.	28	1964	16	41	34.3	7.90S	71.29W	650	332	03	238	52	064	39
5 a	Dec.	1	1967	13	57	02.4	49.47N	154.38E	136	218	14	069	74	310	08
6 a	Mar.	31	1969	19	25	27.2	38.33N	134.60E	417	063	66	214	22	308	05
7 b	Apr.	12	1965	20	41	16.6	30.21N	138.68E	425	161	19	313	69	067	10
8 a	Jan.	2	1965	13	44	19.2	19.11N	145.61E	141	276	20	144	61	013	20
9 a	Feb.	3	1966	5	48	06.1	0.13N	123.46E	131	228	26	104	51	333	29
10 a	Feb.	3	1967	12	30	53.0	5.62S	110.48E	569	118	19	010	44	228	40
11 a	Mar.	24	1967	9	00	19.5	5.98S	112.35E	600	108	00	019	66	199	24
12 a	June	22	1966	20	29	03.6	7.20S	124.59E	507	347	13	238	52	084	35
13 b	Nov.	14	1967	5	28	36.9	5.43S	147.07E	201	288	30	154	50	033	24
14 c	Jan.	7	1968	9	56	40.3	5.07S	153.93E	118	157	18	048	45	261	40
15 d	Dec.	1	1966	4	56	58.2	14.03S	167.10E	132	339	04	245*	48	072	42
16 a	Nov.	4	1968	9	07	38.5	14.18S	172.03E	585	005	18	250	52	106	32
17 a	Dec.	28	1964	16	16	08.7	22.13S	179.62W	577	051	19	243	70	143	04
18 a	Mar.	18	1965	6	22	10.3	19.89S	175.92W	219	018	25	109	03	202	03
19 b	Apr.	10	1965	22	32	46.0	17.84S	178.70W	535	116	44	022	04	288	46
20 b	May	22	1965	10	31	37.3	21.11S	178.50W	538	116	12	224	58	018	30
21 e	Dec.	25	1965	19	20	45.6	18.21S	179.13W	631	094	23	340**	44	202	38
22 a	Mar.	17	1966	15	50	32.2	21.08S	179.18W	626	213	04	304	20	110	70
23 a	July	21	1966	18	30	14.9	17.80S	178.60W	591	112	62	326	24	230	14
24 a	Oct.	2	1967	0	12	52.8	20.96S	178.84W	604	086	12	226	74	354	10
24 b	Oct.	9	1967	17	21	49.5	21.08S	179.35W	654	234	06	087	82	324	04
24 d	Oct.	12	1967	6	35	06.7	21.13S	179.19W	636	220	30	052	60	312	06
25 a	Mar.	14	1965	15	53	06.2	36.42N	70.73E	205	125	00	215	60	035	30

*; The fault plane can not be determined.

**; The fault plane is determined from the foreshock (d) which occurred just before the main shock.

Table 2. Space and time intervals between the main shock and the foreshocks and the aftershocks and the directions of their foci seen from the main shock.

Main Sbock No.	No.	Time Interval hour	min	sec	Distance km	Direction trend	plunge	Main Shock No.	No.	Time Interval hour	min	sec	Distance km	Direction trend	plunge
1 a	b	328	54	45.7	29.5	049	02	17 a	b	113	20	47.6	−17.3	010	65
2 a	b	0	36	10.7	12.9	009	44	18 a	b	171	27	08.6	−11.4	101	03
3 a	b	18	32	56.2	39.9	087	65	19 b	a	−57	41	18.3	30.9	041	39
4 a	b	0	07	55.9	4.0	245	55		c	46	31	56.8	57.2	122	50
5 a	b	285	01	08.9	25.1	150	63		d	211	46	16.5	−22.7	157	23
6 a	b	0	00	03.9	12.3	029	15	20 b	a	−58	59	27.3	−39.2	210	63
7 b	a	−238	19	04.1	−33.5	231	60	21 e	a	−160	59	17.5	−30.6	119	03
8 a	b	4	25	56.8	3.8	238	60		b	−160	22	44.4	−24.8	116	16
9 a	b	264	22	17.3	−88.4	080	44		c	−16	22	46.4	−18.2	145	57
10 a	b	13	40	15.3	−25.9	012	42		d	−1	02	58.9	6.5	42	45
11 a	b	2	45	54.3	3.4	351	36	22 a	b	95	49	15.8	−9.0	330	16
12 a	b	0	00	05.6	17.9	180	27		c	380	40	56.9	8.2	004	12
13 b	a	−20	33	16.2	16.2	356	43		d	394	42	10.6	−27.4	290	46
	c	166	33	05.6	−37.7	302	10	23 a	b	107	14	16.5	30.8	167	31
14 c	a	−309	47	01.4	−38.3	141	32		c	288	55	15.3	−119.4	318	13
	b	−249	28	15.5	−19.9	256	45		d	494	09	52.3	38.8	141	03
	d	289	03	59.1	−56.4	058	56		e	583	42	33.4	−23.3	291	32
	e	320	33	02.9	−91.5	046	75		f	879	57	35.3	−38.7	325	74
15 d	a	−673	27	44.2	123.9	163	03	24 a	b	185	08	55.8	60.6	243	43
	b	−232	24	05.2	227.4	169	14		d	246	22	14.4	51.8	234	45
	c	−30	39	24.5	94.2	162	41	24 b	c	1	12	00.1	−23.1	002	65
	e	152	17	01.3	189.9	166	00		d	61	13	19.4	10.0	090	75
	f	253	00	22.3	109.7	169	00		e	188	47	09.8	−14.0	299	46
	g	349	43	42.3	137.6	159	00	24 d	e	127	33	51.7	−3.6	040	75
	b	388	36	28.8	−88.1	341	13		f	341	17	36.8	−14.7	182	53
	i	416	19	50.1	87.1	156	00	25 a	b	19	20	59.0	−19.3	220	45
	j	1020	58	36.1	110.9	163	01		c	84	45	18.2	−32.7	115	30
	k	1124	20	20.2	−100.0	342	28		d	106	37	55.7	35.6	270	15
16 a	b	1	28	43.1	22.6	342	57								
	c	1	39	32.0	25.4	341	35								

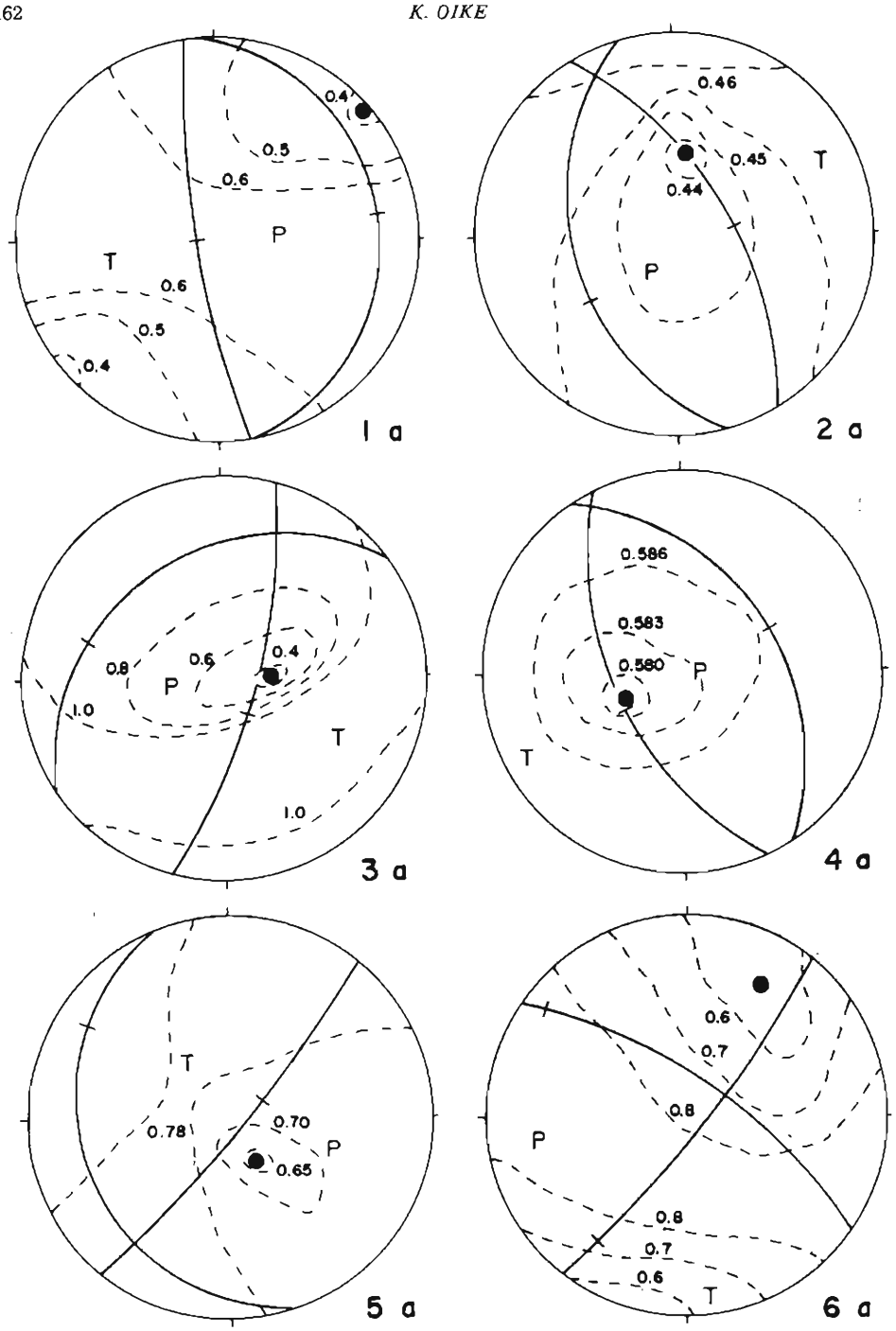

Fig. 6 (a)

Fig. 6. Distribution of foreshocks and aftershocks on the lower hemi-sphere of each main shock indicated by the stereographic projection. Solid circles and triangles indicate the directions and the opposite directions of aftershocks, respectively. Open circles and triangles indicate those of foreshocks. Values of dotted lines show the standard deviations in seconds.

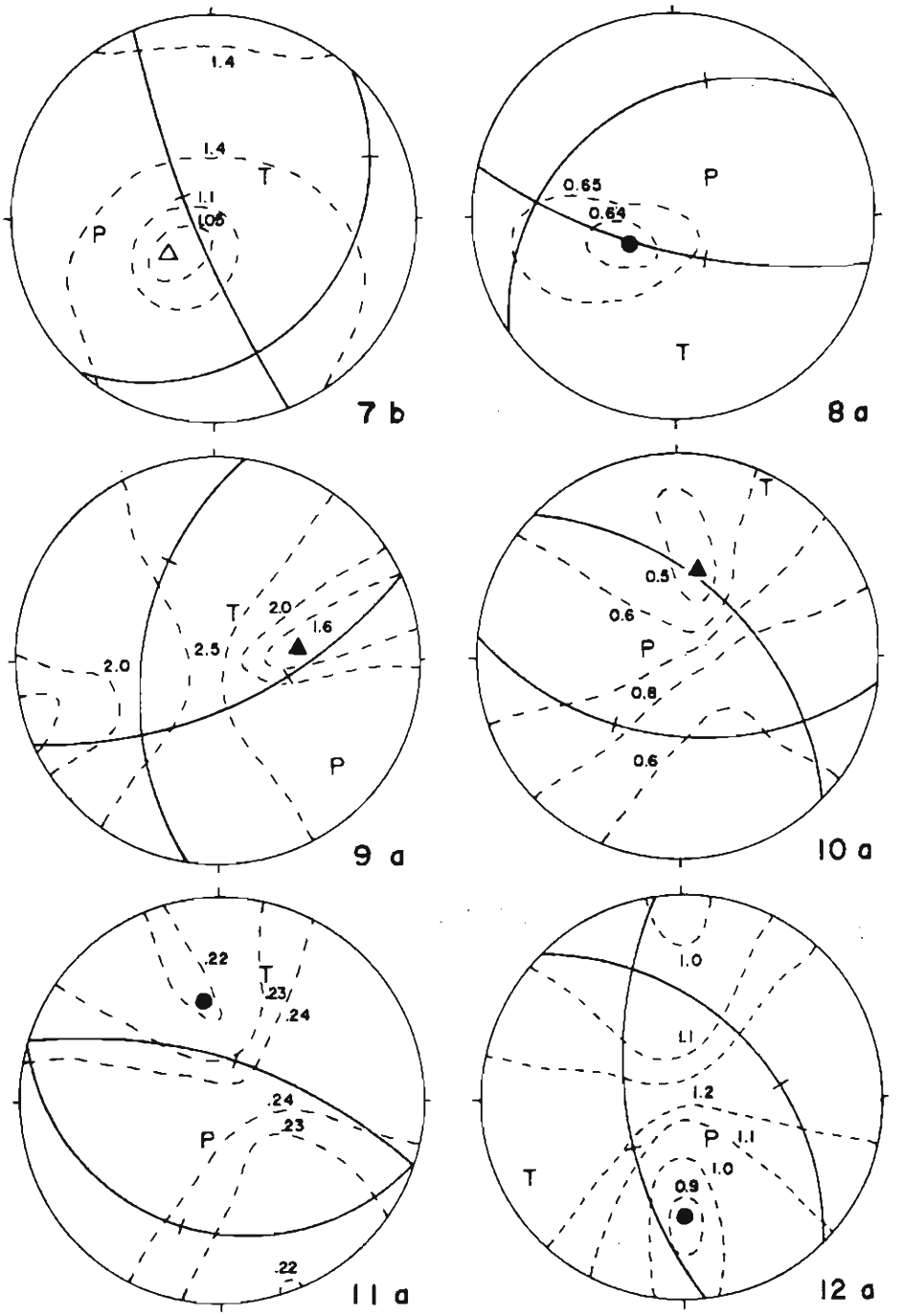
1.4
1.4
T
1.1
1.05
P
7 b
0.65
0.64
P
T
8 a
T
2.0
1.6
2.5
2.0
P
9 a
T
0.5
0.6
P
0.8
0.6
10 a
.22
T
.23/
.24
.24
.23
P
.22
11 a
1.0
1.1
1.2
P
1.1
1.0
0.9
T
12 a

Fig. 6 (b)

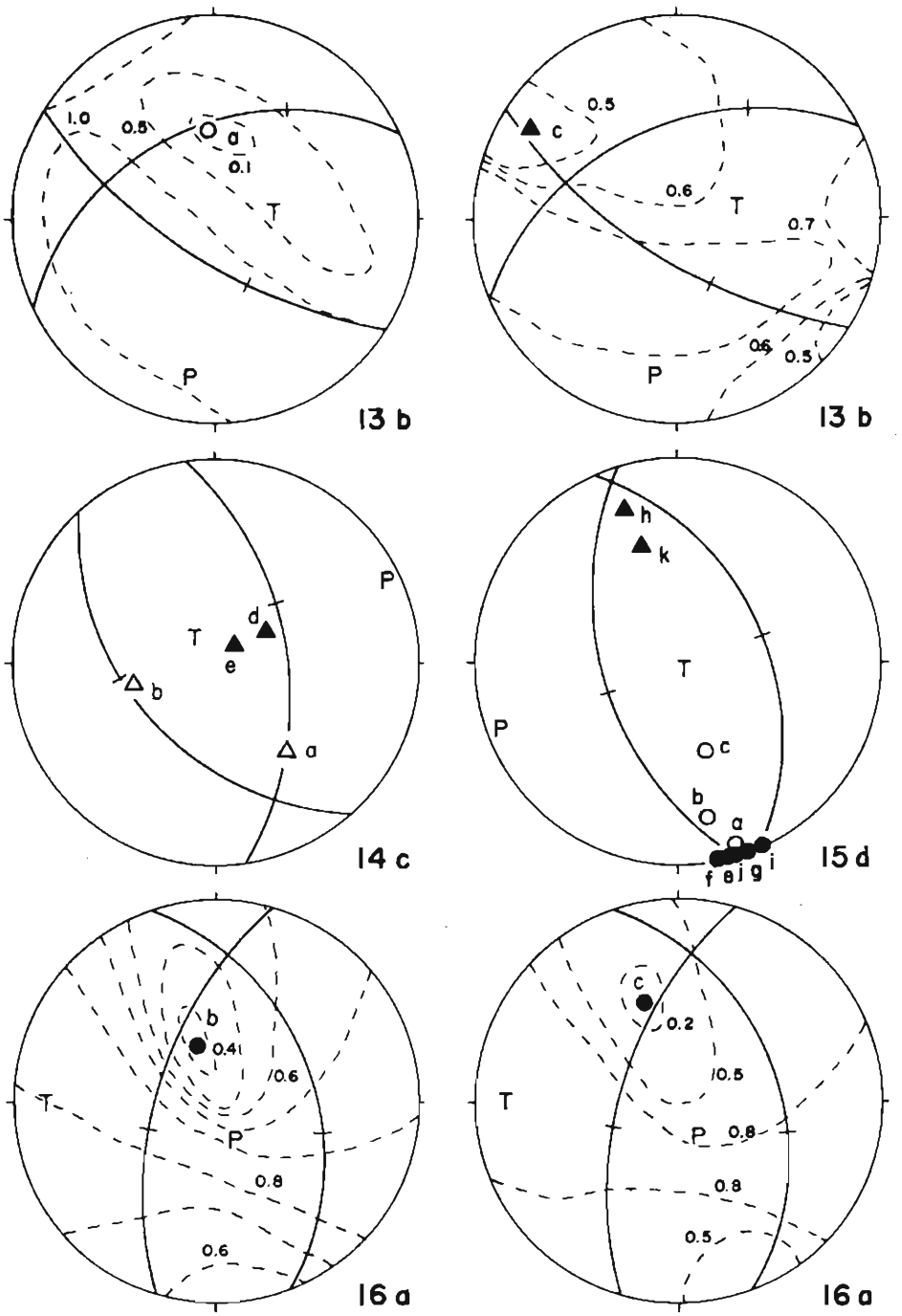
1.0
0.8
a
0.1
T
P
13 b
0.5
c
0.6
T
0.7
0.6
0.5
P
13 b
P
d
T
e
b
a
14 c
h
k
T
P
c
b
a
f e i g i
15 d
c
0.2
0.5
T
P
0.8
0.8
0.5
16 a
b
0.4
0.6
T
P
0.8
0.6
16 a

Fig. 6 (c)

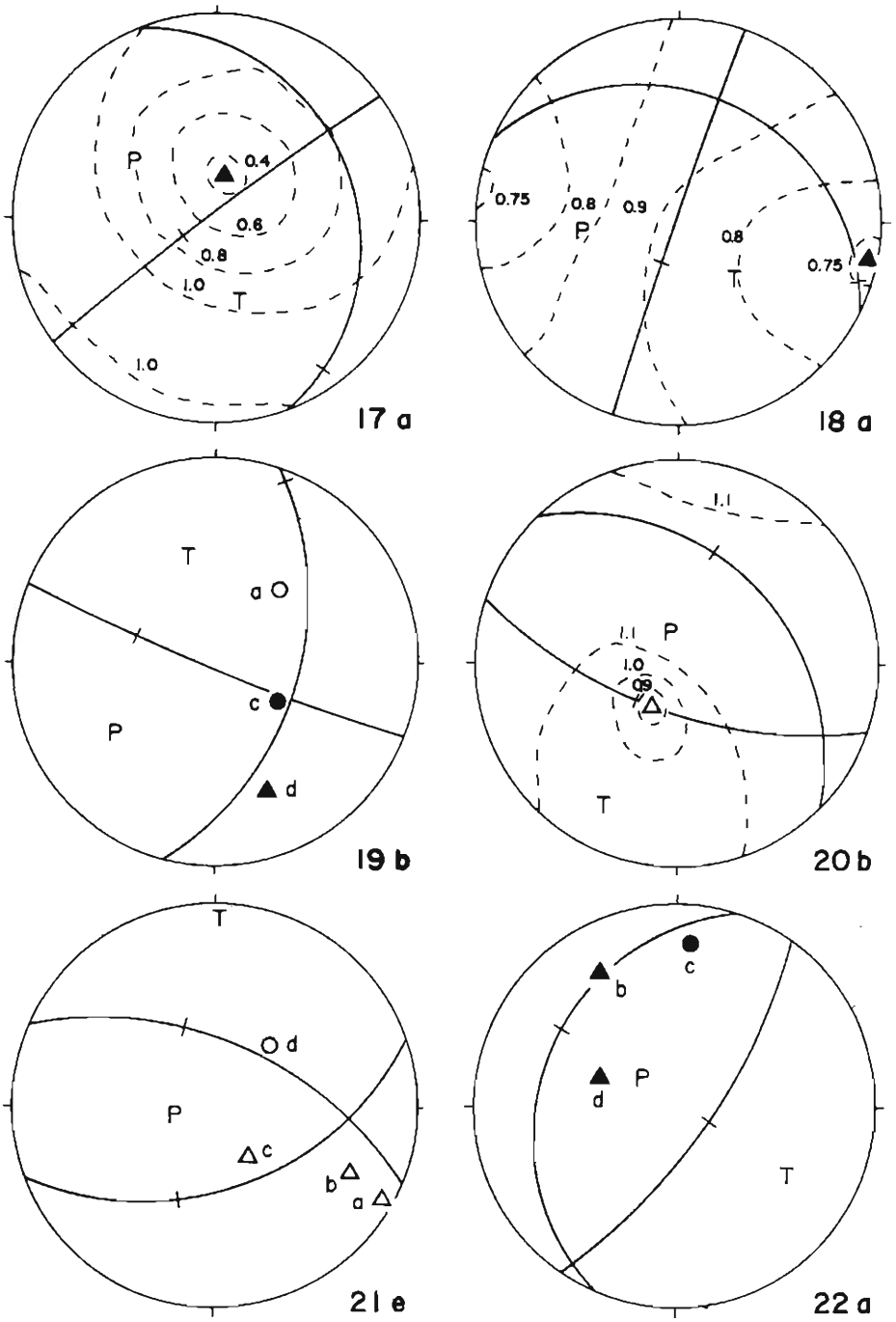
P
0.4
0.6
0.8
1.0
T
1.0
17 a
0.75
0.8
0.9
P
0.8
T
0.75
18 a
T
a
c
P
d
19 b
1.1
1.1
P
1.0
0.9
T
20 b
T
d
P
c
b
a
21 e
b
c
d
P
T
22 a

Fig. 6 (d)

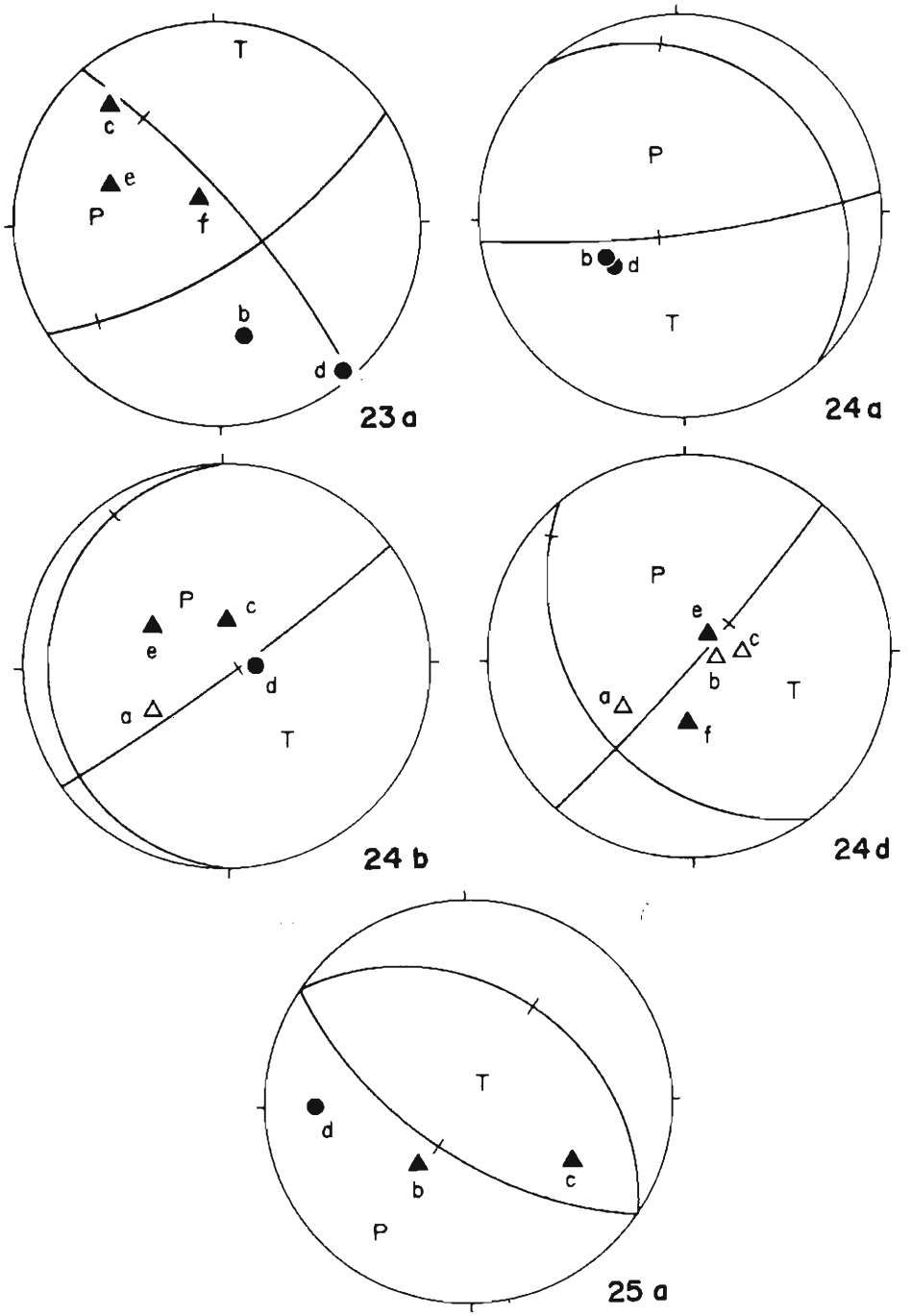

Fig. 6 (e)

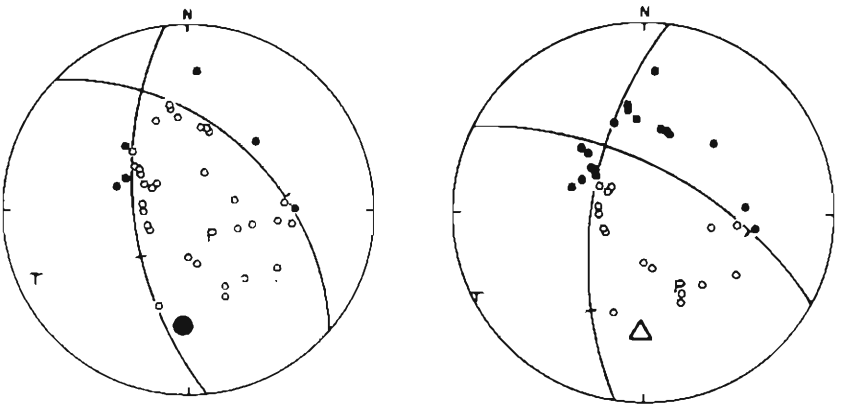

Fig. 7. Fault plane solutions of the first (left) and the second (right) shocks and their mutual directions of the doublet of June 22, 1966.

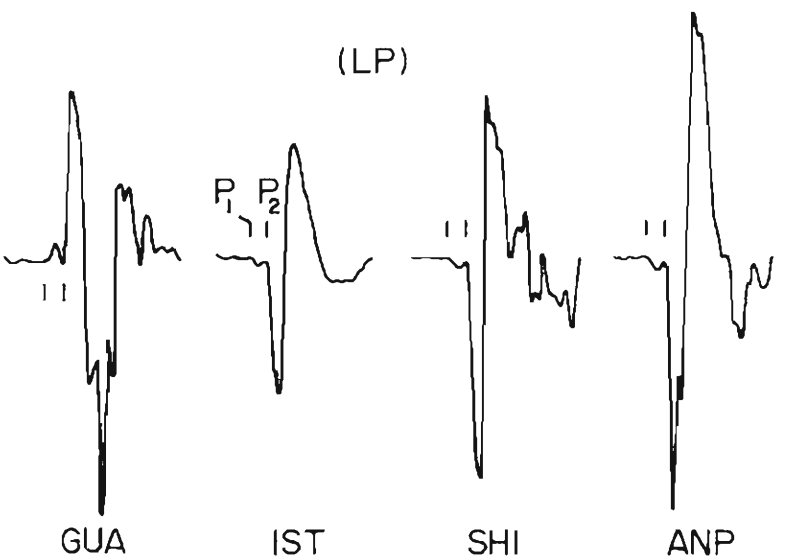

Fig. 8. Long-period P waves of the doublet of March 31, 1969.

was also a doublet with a remarkably short time interval. Four examples of the long-period P wave forms recorded by the WWSSN are shown in Fig. 8. Median-period records obtained at Dodaira (DDR) and some examples of the short-period records obtained at the microearthquake observation stations in Japan are shown in Fig. 9. Comparing these wave forms with the records of other normal shocks of the same depth and the same epicentral distance, it is clearly found that this earthquake consisted of two shocks occuring successively near the foci.

Time differences between two P phases read from these seismograms at 29 stations are listed in Table 3. Stations whose epicentral distances are less than 10 degrees in the upper half of the table are mainly the microearthquake observation stations

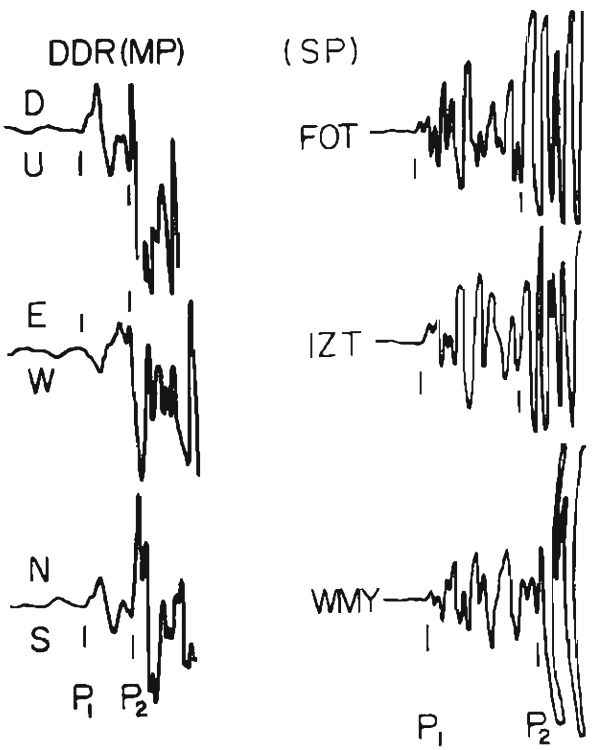

Fig. 9. P wave forms of the doublet of March 31, 1969, recorded by the median-period and short-period seismographs.

in Japan and others belong to the WWSSN. The fault plane solution of the first shock seems to coincide with that of the second shock because there are no stations at which the initial P motions of two shocks have distinctly opposite directions.

The second shock of this doublet has been analyzed by Mikumo (1971)[34]. He determined the slip plane of the shock from the distribution of pulse width of corrected long-period P waves and calculated the various parameters of the fault plane. In Fig. 10, the radiation patterns of P waves of the first and second shocks with nodal lines referred to his solution. The direction of $\overline{O_1O_2}$ obtained from the distribution of τ_j is also plotted.

One of the nodal planes whose strike was in the north-south direction was determined to be a slip plane from the results in Fig. 10, which coincides with the Mikumo's (1971)[34] results. The length of the fault plane obtained by him was 10–14 km and the distance between two foci obtained from the analyses of the doublet was 12.3 $\pm$1.9 km.

If the time interval from the end of the fault propagation of the first shock to the second shock is negligibly small, the propagating velocity of the fracture can be determined from the space and time intervals of multiplets. The relation between them containing the data obtained by Chandra (1970)[35] and Fukao (1971)[36] is shown in Fig. 11. The line of 4.7 km/sec in Fig. 11 shows the upper limit of the propagating velocity obtained from the present data for deep earthquakes.

Table 3. Polarities of two P phases and the time intervals between them, observed for the deep earthquake of March 31, 1969, in the Sea of Japan.

Station	Azimuth (deg)	Δ (deg)	t_{p1} m	t_{p1} s	Polarity P_1	Polarity P_2	τ (sec)
KMU	58	7.48	27	14.7	D		3.2
AOB	91	4.91	26	50.0	D	D	3.0
MAT	122	3.38	26	34.6	D	(D)	3.9
DDR	123	4.34	26	41.6	D	D	3.7
ISE	156	4.25	26	42.7	(D)		4.0
HMT	168	3.17	26	32.8	C		5.2
WKU	174	4.17	26	41.9	C		5.0
IZT	176	3.37	26	34.8	C	(C)	4.5
OYT	179	3.00	26	34.0	C		4.6
MZT	182	3.35	26	34.8	C	(C)	4.8
FOT	185	3.01	26	31.9	C		5.2
TTT	186	2.83	26		C	C	5.8
WMY	189	4.75	26	47.7	C	(D)	5.5
IHR	191	4.73	26	47.5	C	(D)	5.5
SHK	202	4.10	26	41.9	C	C	5.1
ALQ	46	87.74	37	34.5	(C)	C	(2.2)
HNR	148	53.07	34	06.0	C	C	4.3
RAB	155	45.33	33	08.0	C	C	4.8
GUA	157	26.33	30	28.0	C	C	5.2
PMG	163	48.91	33	34.0	C	C	4.3
MAN	211	26.43	30	37.0	(D)	D	(3.7)
ANP	224	17.17	29	08.0	D	D	3.7
SNG	233	43.63			D	D	4.7
CHG	248	36.55			D	D	4.7
KBL	287	51.89			D	D	3.3
SHI	290	66.53	35	33.3	D	D	3.2
JER	301	77.64	36	43.0	D	D	3.5
TAB	301	66.56	35	34.0	D	D	4.0
IST	311	75.89	36	32.8	D	D	3.5

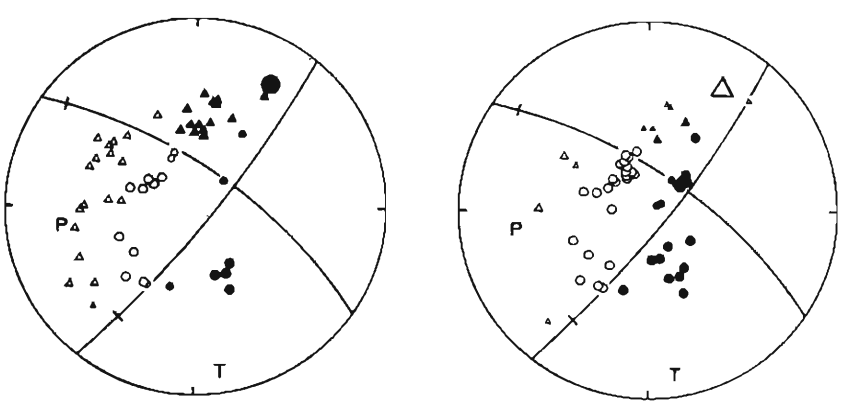

Fig. 10. Fault plane solutions of the first (left) and the second (right) shocks and their mutual directions of the doublet of March 31, 1969.

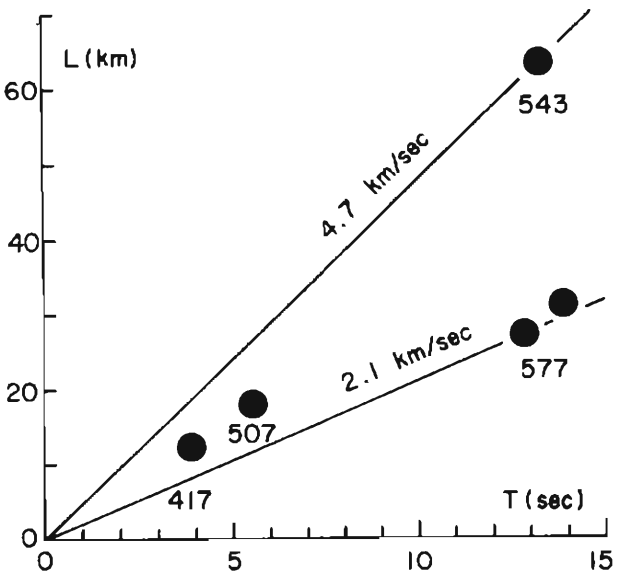

Fig. 11. Propagating velocity of the fault determined from the time and space intervals of two shocks in doublets and a triplet.

5. Relation Between the Focal Mechanism and the Distribution of Foci in the Multiplets

The multiplets except two doublets already mentioned have larger time intervals and are clearly separated in the records and the bulletins. No clear patterns such as foreshocks, a main shock and aftershocks as is seen in the case of shallow earthquakes are discovered in the time sequences of intermediate and deep multiplets. In this paper, shocks before and after a large shock are called foreshocks and aftershocks, respectively.

As is shown in Fig. 6 and Table 2, the foci of foreshocks and aftershocks distribute on one of the nodal planes of a main shock in almost all cases. It is remarkable that in case containing more than two aftershocks they occur on an identical nodal plane. It suggests that the aftershocks occur by the propagation of the fault plane of the main shock.

The multiplets of Nos. 1–12, 17, 18 and 20 are doublets. Among them Nos. 7 and 20 have small first shocks and others have small aftershocks. Their foci are on one of the nodal planes of main shocks with no exceptions, and from it the slip plane of each main shock is determined.

No. 16 is a triplet with two aftershocks. They distribute on an identical nodal plane of the main shock and have nearly the same directions and distances from the main shock.

Foreshocks and sftershocks of Nos. 19, 24b and 24d distribute on an identical nodal plane of main shocks. But one of the small foreshocks of Nos. 13 and 14 is on another nodal plane. In these two cases a small foreshock is not a trigger directly affected to the occurrence of the main shock. But aftershocks always distribute on a fault plane of the main shock.

Multiplet of No. 21 has many foreshocks, which distribute on a nodal plane except only one. The foreshock (d) just before the occurrence of the main shock with a time interval of about 1 hour is the trigger of the main shock.

Nos. 14, 19, and 22–25 have many aftershocks which distribute on one of the nodal planes of the main shock. Many foreshocks and aftershocks of No. 15 flock together in the direction of the null axis of the main shock with comparaitvely large space intervals. These shocks of 15a–15k seem to be contained in a multiplet considering the normal seismic activity in this region, but the main shock is remarkably large compared with other shocks.

For Nos. 4, 12 and 24, fault plane solutions of more than two shocks are obtained. In No. 24 the relation between fault plane solutions and the distribution of aftershocks suggest that the dip slip type fault plane propagated itself downward in order of a, b and d being gradually distorted, and the strike of the fault plane became parallel to those of other multiplets in the same region in the last stage of propagation. In those three solutions the axes of the compressional stress lie in the same direction along the dip of the seismic plane. Nos. 4a and 4b have the same radiation patterns of P waves, and the second shock occurs in the direction of the pole of the fault plane of the first shock.

The frequency distribution of the angles of the directions of aftershock foci seen from the pole of the fault plane is shown in Fig. 12, except No. 15. They distribute most frequently around the pole in both cases of intermediate and deep earthquakes. The component of τ_{xy} is increased in all directions along the edge of a fault plane as is shown in Fig. 4. If results that the aftershocks have a tendency to occur in the direction of the pole is reliable, it suggests the properties of the initial stress field, otherwise it will be necessary to correct the fault model, for example, to give a large ratio of a/b.

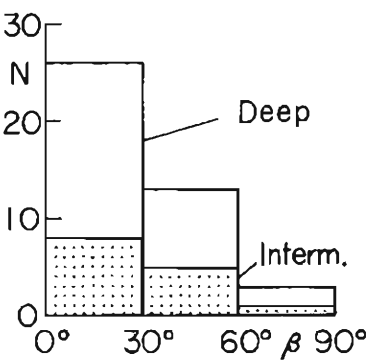

Fig. 12. Frequency distribution of the angles between the direction of after-shock foci and the poles of the fault planes of the main shocks.

6. Distribution of Slip Planes Within the Descending Slab of Lithosphere

Slip planes determined above are compared with the contours of hypocentral depth on the maps of some regions in Figs. 14–18. These contours refer to Isacks and Molnar (1971)[37]. It is generally concluded that for each multipelt the nodal

plane which is parallel to the contour lines of hypocentral depth in the region where the multiplet occurred is determined to be the slip plane.

Taking into consideration the fact mentioned above, the slip planes in the regions where the earthquakes are generated by the stress field of down-dip extension along the seismic plane are classified into two types of A and B in Fig. 13, and those in the regions of down-dip compression are classified into C and D types in Fig. 13.

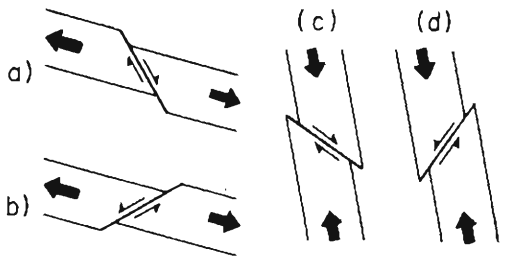

Fig. 13. Types of slip planes in the intermediate (a and b) and the deep (c and d) regions.

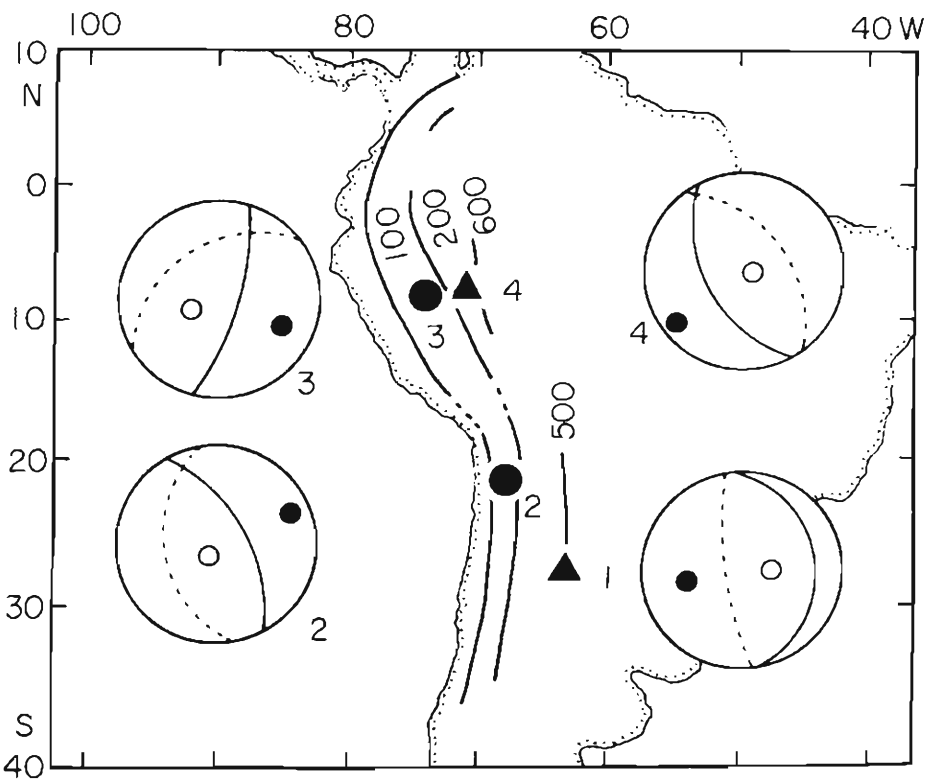

Fig. 14. Distribution of slip planes in the South America region. Solid circles and triangles on the map indicate the epicenters of intermediate and deep shocks, respectively. Solid lines are the contours of hypocentral depths. In the stereographic projection of the lower hemi-sphere of each focus, open and closed circles indicate the axes of compression and extension, and solid and dotted lines indicate the fault and auxiliary planes, respectively.

(a) South America

The results are shown in Fig. 14. There are two pairs of intermediate and deep multiplets. Intermediate earthquakes, Nos. 2 and 3, have the slip planes of A type and two deep earthquakes, Nos. 1 and 4, show C and D types, respectively. The location and the radiation pattern of the large deep earthquake analyzed by Fukao (1971)[38] are similar to those of No. 4 earthquake but its slip plane is C type. On the deep earthquake studied by Chandra (1970)[39] the results are nearly the same as those of No. 4.

(b) Japan and its vicinity

The results are shown in Fig. 15. The slip planes of Nos. 5–7 are parallel to the contour lines. This coincides with the Mikumo's (1971)[40] results on Nos. 4 and 5 earthquakes in his paper. The slip plane of the No. 8 earthquake is also parallel to the contour because in the Mariana region the seismic plane curves along the trench (Katsumata and Sykes, 1969)[41]. The direction of two slip planes of two earthquakes in the southern end of Izu-Ogasawara trench obtained by Mikumo (1971) coincide

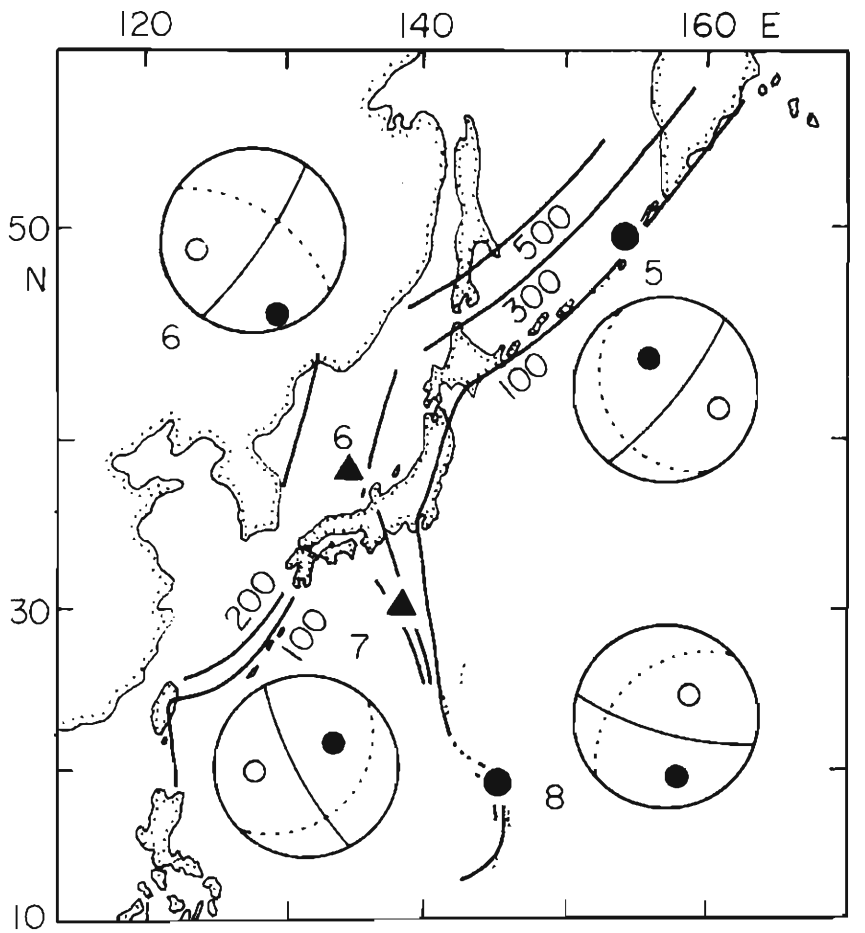

Fig. 15. Results in and around Japan. Expressions are same as in Fig. 14.

well with that of No. 8 in our results, and so this nearly east-west direction of the strike of the slip planes in this region seems to have a close relation to the stress field within the gradually distorted lithospheric plate.

Intermediate earthquakes in this region have also the slip planes of A type in Fig. 13.

(c) Indonesia

The results in this region are shown in Fig. 16. The slip plane of No. 9 earthquake is determined parallel to the contour line which curves suddenly in this region (Fitch,

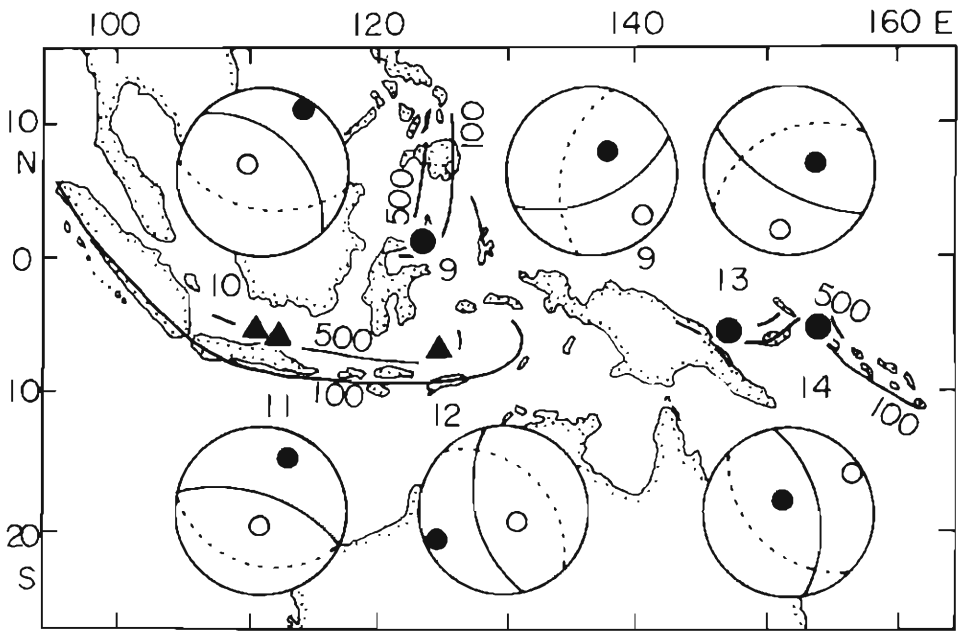

Fig. 16. Results in the Indonesia region. Expressions are same as in Fig. 14.

1970)[42]. The slip planes of C type of two deep earthquakes in the Java Sea (Nos. 10 and 11) are parallel to the contour lines. No. 12 in the Banda Sea has the same direction of compressional stress axis as two deep shocks in the Java Sea but has the slip plane in the north-south direction parallel to the contour lines in the Banda Sea region. It suggest that the focal mechanism of deep earthquakes in this region is greatly affected by the curvature of the seismic zone beneath the Banda Sea as is discussed from the distribution of the principal axes of stresses by Fitch and Molnar (1970)[43].

(d) Melanesia

The results are shown in Fig. 17. No. 13 in the Bismark Sea has the A type slip plane parallel to the contour. No. 14 in the Bougainville Island has the slip plane parallel to the contour but the T-axis is nearly vertical and it shows the gravitaional body forces cause down-dip extension in the slab (Isacks and Molnar, 1971)[44].

Aftershocks of No. 15 distribute in the direction of null axis of the main shock which coincides with the direction of the contour lines and the slip plane can not be determined. But the dip-slip type solution is obtained and the T-axis lies along the dip of the seismic plane.

Many multiplets are found in the Tonga region and only the results with very small deviations are shown in Fig. 17. The slip palnes of Nos. 17, 19 and 22 are parallel to the contours and that of last stage of No. 24 shows a similar result. Many

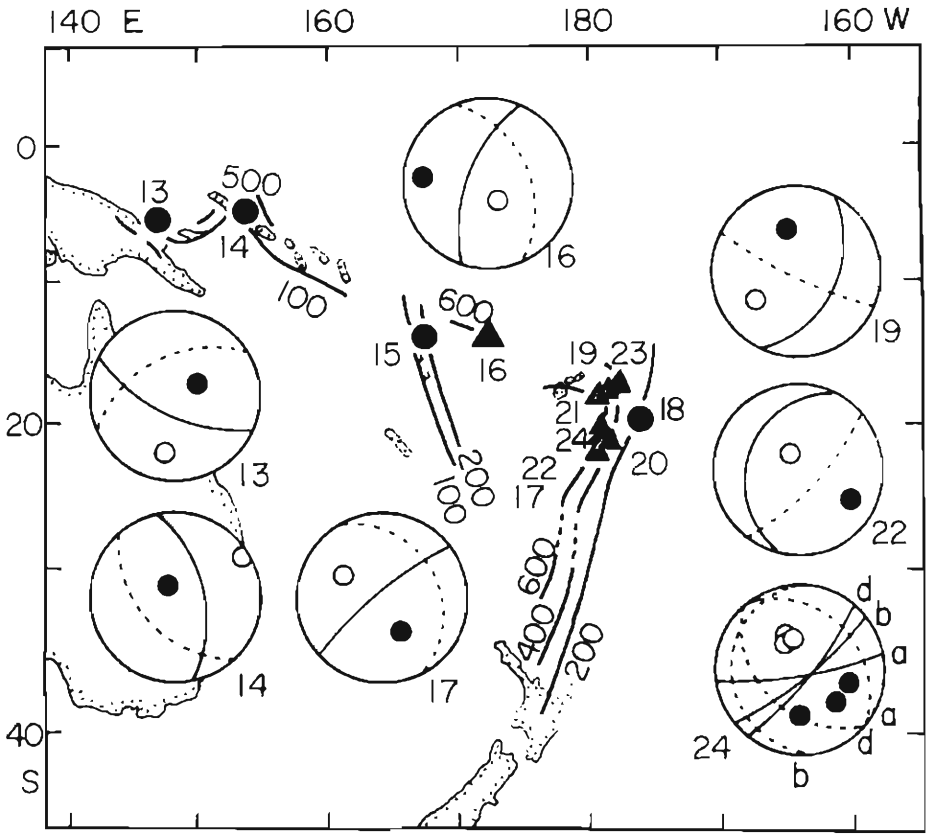

Fig. 17. Results in the Melanesia region.

aftershocks of No. 23 near the Fiji Islands distribute on the nodal plane whose strike is in the NW–SE direction and the fault plane solution of this earthquake is a strike slip type. No. 19 in the same region shows similar characters as No. 23. These correspond to the fact that in a region of marked contortion the lithosphere is significantly deformed.

(e) Hindu-Kush

The results of an intermediate multiplet are shown in Fig. 18. Thc slip plane of A type are obtained in the same way as in the other regions.

(f) Types of slip planes

The slip planes of 25 earthquakes are classified according to four types in Fig. 13 as is shown in Table 4.

If A type slip planes are generated frequently within the intermediate depth of the lithosphere in the region where its dip angle is not so large, for example, beneath the Japanese Islands, the lithospheric plate will be deformed gradually to become a

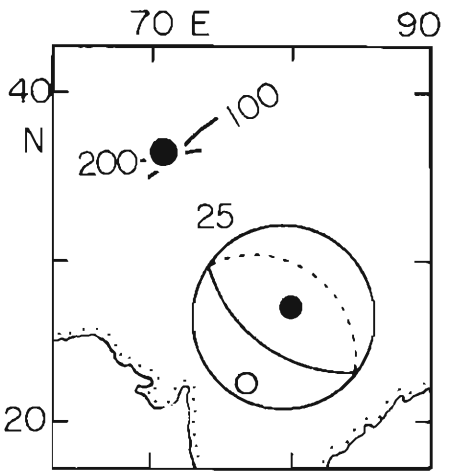

Fig. 18. Results in the Hindu-Kush region.

Table 4. Distribution of the types of slip planes classified according to Fig. 13.

	Intermediate Earthq.			Deep Earthq.		
Type	a	b	?	c	d	?
Number	8	0	2	6	8	1

downward warping feature as is seen in the 100–200 km depth in the Izu-Mariana region (Katsumata and Sykes, 1969)[45].

In the deep region where the stress of down-dip compression is predominant, two types of slip plane are equally generated.

7. Discussions

The shear fault model which is described as the distribution on the fault surface of the shear dislocations equivalent to the double couple force is most approapriate to explain the various kinds of seismological data concerned with the focal mechanisms. Some characteristics of the intermediate and deep multiplets presented in this study are also explained by the application of the shear fault model. But the question still remaining is that the intermediate and deep earthquakes are seldom accompanied by foreshocks and aftershocks which is in striking contrast to the shallow earthquakes.

This difference may depend partly upon the detection capability of the observation networks and partly upon the difference in the nature of the seismic activity due to the difference of the physical conditions of the focal regions. It is possible to consider that the residual stress field around the shallow earthquakes is remarkably complicated because of the existence of the free boundary and the complex crustal structures. The source model of intermediate and deep earthquakes, though it is somewhat different from that of shallow earthquakes, must of cause explain the radiation pattern of double couple type and moreover the various characteristics of the multiplets,

In the regions of the edge, the marked contortion and the triple junction of the lithospheric plates, many multiplets are found. By observing the original records atten-

tively, more doublets and triplets with very short time intervals will be found, and significant information on the nature of the complicated features of the seismic zones in these regions and on the focal mechanisms of intermediate and deep earthquakes will be obtained by analyzing them.

Acknowledgment

The author wishes to thank Drs. Yoshimichi Kishimoto and Takeshi Mikumo for their valuable discussions and suggestions. Copies of seismograms were kindly provided from many observation stations in Japan. Computations were made on a FACOM 230–60 at the Data Processing Center, Kyoto University.

References

1) Oike, K.: On the Nature of the Occurrence of Intermediate and Deep Earthquakes. 2. Spatial and Temporal Clustering, Bull. Disast. Prev. Res. Inst., Vol. 21, Part 1, 1971, (in press).
2) Knopoff, L. and M. J. Randall: The Compensated Linear-Vector Dipole: A Possible Mechanism for Deep Earthquakes, J. Geophys. Res., Vol. 75, 1970, pp. 4957–4963.
3) Randall, M. J. and L. Knopoff: The Mechanism at the Focus of Deep Earthquakes, J. Geophys Res., Vol. 75, 1970, pp. 4965–4976.
4) Isacks, B. and P. Molnar: Mantle Earthquake Mechanism and the Sinking of the Lithosphere, Nature, Vol. 223, 1969, pp. 1121–1124.
5) Isacks, B. and P. Molnar: Distribution of Stresses in the Descending Lithosphere from a Global Survey of Focal Mechanism Solutions of Mantle Earthquakes, Rev. Geophys., Vol. 9, 1971, pp. 103–174.
6) McKenzie, D. P.: Speculations on the Consequences and Causes of Plate Motions, Geophys. J., Vol. 18, 1969, pp. 1–32.
7) loc. cit. 4).
8) Fukao, Y.: Focal Process of a Deep-Focus Earthquakes as Deduced from Long-Period P and S Waves, Bull. Earthq. Res. Inst., Vol. 48, 1970, pp. 707–727.
9) Mikumo, T.: Source Process of Intermediate-Depth Earthquakes as Inferred from Long-Period P and S Wave Forms, 1. Intermediate-Depth Earthquakes in the Southwest Pacific Region, J. Phys. Earth, Vol. 19, 1971, pp. 1–19.
10) Abe, K.: Source Studies of Intermediate-Depth Earthquakes Based on Long-Period Seismic Waves, 1. The South Sandwich Islands Earthquake of May 26, 1964, Phys. Earth Planet. Interiors, 1971, (in press).
11) Oike, K.: The Deep Earthquake of June 22, 1966 in Banda Sea: A Multiple Shock, Bull. Disast. Prev. Res. Inst., Vol. 19, 1969, pp. 55–65.
12) Chandra, U.: The Peru-Bolivia Border Earthquake of August 15, 1963, Bull. Seism. Soc. Amer., Vol. 60, 1970, pp. 639–646.
13) Fukao, Y.: Focal Process of A Large Deep-Focus Earthquake as Inferred from Long-Period P Waves——The Western Brazil Earthquake of 1963——, Phys. Earth Planet. Interiors, 1971, (in press).
14) Isacks, B. L., L. R. Sykes and J. Oliver: Spatial and Temporal Clustering of Deep and Shallow Earthquakes in the Fiji-Tonga-Kermadec Region, Bull. Seism. Soc. Amer., Vol. 57, 1967 pp. 935–958.
15) Santô, T.: Characteristics of Seismicity in South America, Bull. Earthq. Res. Inst., Vol. 47, 1969, pp. 635–672.
16) Santô, T.: Regional Study on the Characteristic Seismicity of the World. Part II. From Burma Down to Java, Bull. Earthq. Res. Inst., Vol. 47, 1969, pp. 1049–1061.

17) Santô, T.: Regional Study on the Characteristic Seismicity of the World. Part III. New Hebrides Islands Region, Bull. Earthq. Res. Inst., Vol. 48, 1970, pp. 1–18.
18) Santô, T.: Regional Study on the Characteristic Seismicity of the World. Part IV. New Britain Island Region, Bull. Earthq. Res. Inst., Vol. 48, 1970, pp. 127–143.
19) Yamakawa, N.: Aftershocks and Focal Mechanism of Main Shocks, Goephys. Mag., Vol. 36, 1971, (in press).
20) Yamakawa, N. and M. Kishio: Aftershocks of the Tokachi-Oki Earthquake of 1968 (I), Geophys. Mag., Vol. 36, 1971, (in press).
21) Chinnery, M. A.: The Stress Changes That Accompany Strike-Slip Faulting, Bull. Seism. Soc. Amer., Vol. 53, 1963, pp. 921–932.
22) Maruyama, T.: Stress Fields in the Neighborhood of a Crack, Bull. Earthq. Res. Inst., Vol. 47, 1969, pp. 1–29.
23) Eshelby, J. D.: The Determination of the Elastic Field of an Ellipsoidal Inclusion and Related Problems, Proc. Roy. Soc. (London), A, Vol. 241, 1957, pp. 376–396.
24) Savage, J. C.: Radiation from a Realistic Model of Faulting, Bull. Seism. Soc. Amer., Vol. 56, 1966, pp. 577–592.
25) Maruyama, T.: Statical Elastic Dislocations in an Infinite and Semi-Infinite Medium, Bull. Earthq. Res. Inst., Vol. 42, 1964, pp. 289–368.
26) loc. cit. 21).
27) Oike, K.: Distribution of Stresses and Dynamic Displacements Around a Fault, J. Seism. Soc. Japan, Vol. 24, 1971, (in press).
28) Haskell, N. A.: Elastic Displacements in the Near-Field of a Propagating Fault, Bull. Seism. Soc. Amer., Vol. 59, 1969, pp. 865–908.
29) Oike, K., M. Koizumi and N. Hirano: Continuous Observation by Strain Seismographs and Tiltmeters of Variable Capacitance Type, Annuals Disast. Prev. Res. Inst., No. 12A, 1969, pp. 145–154.
30) loc. cit. 5).
31) loc. cit. 14).
32) loc. cit. 11).
33) loc. cit. 11).
34) Mikumo, T.: Source Process of Deep and Intermediate Earthquakes as Inferred from Long-Period P and S Waveforms. 2. Deep and Intermediate Earthquakes around Japan, J. Phys. Earth, Vol. 19, 1971, (in press).
35) loc. cit. 12).
36) loc. cit. 13).
37) loc. cit. 5).
38) loc. cit. 13).
39) loc. cit. 12).
40) loc. cit. 34).
41) Katsumata, M. and L. R. Sykes: Seismicity and Tectonics of the Western Pacific: Izu-Mariana-Caroline and Ryukyu-Taiwan Regions, J. Geophys. Res., Vol. 74, 1969, pp. 5923–5948.
42) Fitch, T. J.: Earthquake Mechanisms and Island Arc Tectonics in the Indonesian-Philippine Region, Bull. Seism. Soc. Amer., Vol. 60, 1970, pp. 565–591.
43) Fitch, T. J. and P. Molnar: Focal Mechanisms along Inclined Earthquake Zones in the Indonesia-Philippine Region, J. Geophys. Res., Vol. 75, 1970, pp. 1431–1444.
44) loc. cit. 5).
45) loc. cit. 41).